Soft Matter

Accepted Manuscript

ROYAL SOCIETY OF CHEMISTRY

www.rsc.org/softmatter

Table of Contents

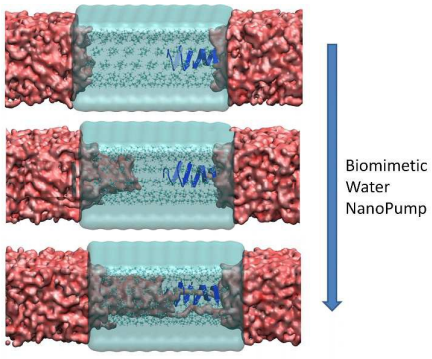

The functionalization of a dried narrow hydrophobic nanopore by a protein channel completely restores the nanopore wetting. The protein acts as a water nanopump when confined inside this nanopore.

Biomimetic Solution Against Dewetting in Highly Hydrophobic Nanopore

Fabien Picaud[1], Guillaume Paris[1], Tijani Gharbi[1], Sébastien Balme[2], Mathilde Lepoitevin[2], Vidhyadevi Tangaraj[2], Mikhael Bechelany[2], Jean Marc Janot[2], Emmanuel Balanzat[3], François Henn[4]*

[1] Laboratoire de Nanomédecine, Imagerie et Thérapeutique, EA 4662, Université Bourgogne Franche-Comté, Centre Hospitalier Universitaire de Besançon, 16 route de Gray, 25030 Besançon cedex, France

[2] Institut Européen des Membranes, UMR5635 CNRS-UM2-ENSCM, Place Eugène Bataillon, 34095 Montpellier cedex 5, France

[3] Centre de recherche sur les Ions, les Matériaux et la Photonique, UMR6252 CEA-CNRS-ENSICAEN, 6 Boulevard du Maréchal Juin, 14050 Caen Cedex 4, France

[4] Equipe Nanostructures et spectroscopies, Laboratoire Charles Coulomb, UMR5221 CNRS-UM2, Place Eugène Bataillon, 34095 Montpellier cedex 5, France

Corresponding author: fabien.picaud@univ-fcomte.fr

Abstract

A water molecule is the foundation of life and symbolizes the primary compound in every living system. While many of its properties are understood in bulk solvent, its behavior in a small hydrophobic nanopore still raises fundamental questions. For instance, a wetting/dewetting transition in a hydrophobic solid-state or polymer nanopore occurs stochastically and can only be prevented by

external physical stimuli. Controlling these transitions would be a primary requirement to improve many applications. Some biological channels, such as gramicidin A (gA) proteins, show a high rate of water and ion diffusion in their central subnanochannel while their external surface is highly hydrophobic. The diameter of this channel is significantly smaller than the inner size of the lowest artificial nanopore in which water drying occurs (i.e. 1.4nm). In this paper, we propose an innovative idea to generate nanopore wetting as a result of which the application of an external field is no longer required. In a nanopore, the drying or wetting of the inner walls occurs randomly (in experiments and in simulations). However, we have shown how the confinement of gA, in a dried hydrophobic nanopore, rapidly generates a stable wetting of the latter. We believe that this simple idea, based on biomimetism, could represent a real breakthrough that could help to improve and develop new nanoscale applications.

KEYWORDS: nanopore; simulations; biomimetism; transition phase; patch-clamp.

INTRODUCTION

Water is the main motor for life [1-3]. Without water, all organisms would disappear progressively. Water molecules play an essential role as a solvent for ion diffusion, as an active candidate for enzymatic and chemical reactions, or as a pressure regulator in cells by filling accessible cavities. While mainly considered as a motor of life, its behavior is still far from being fully understood and may show some peculiarities depending on its action. For instance, water can surround ions and thus create a so-called hydration shell to limit the strong electrical interactions between the ions, which makes their diffusion possible. Proteins, such as ionic channels, have a particular area, called a filter, where specific ions and water molecules can diffuse in a single-file chain configuration. The energetic cost due to the total or partial desolvation of the diffusing ion in this selective filter is then compensated by the binding of the ion to specific functional groups of the protein. In such cases, water can spontaneaously adapt to its environment to follow ions and allow selectivity. Furthermore, the natural selectivity and permeability of these specific proteins, such as KcsA, gA, etc. are so high that they were never achieved at the same time in artificial nanopores. At present, this represents a

fundamental scientific challenge, especially for the desalination of seawater[4] and dialysis[5]. While considerable progress has been made since the beginning of the 21th century[6] by developing solid-state nanopores based on single-wall carbon nanotubes[7],[6] (SWCNT), boron nitride nanotubes[8] (t-BNNT), PDMS-glass[9], Silicon Nitride[10] and polymeric track-etched method[11], their ionic selectivity still requires either a significant electric field (high cost) or a very small nanopore size, which strongly hinders permeability. This technology has not been developed mainly due to the fact that desolvation and water diffusion phenomena are extremely difficult to control in a nanopore. The internal diameter of this nanopore (radius up to 1 nm) is at the origin of a water transition state that changes between vapor and liquid phases over time. This "so-called" wetting/dewetting transition was firstly emphasized and described in literature by using molecular dynamic (MD) simulations. The dewetting was also discussed as it was considered as being the cause for the loss of ionic conductivity and was thus related to the pore gating mechanism in hydrophobic nanopores[12-14]. For example, Beckstein et al.[15, 16] highlighted a distinct two-state regime in hydrophobic nanotubes of varying radii which involved some major changes in the predicted theoretical ion diffusion. This study showed that the energy required to wet the internal hydrophobic surface of the nanopore could be so high that this could explain why, in experiments, pressures could break the fragile nanostructure. Close to hydrophobic surfaces, the variation of the water density is significant and can yield a lower density than in normal volume conditions[17]. If water is confined in a small hydrophobic nanopore, it can be released from the pore and can spontaneously evaporate[18, 19]. Hydrophobic nanopore walls could therefore create a gate system for water, which could involve major consequences such as hindering the development of the application. Macromolecule or nanoparticle detection processes could be affected by this gate system[20, 21]. Macromolecule translocation through the nanopore is detected by ionic measurement via application of a voltage. The gate phenomenon, combined with the current fluctuations induced by the macromolecule translocation, could affect the measurement.

To overcome this problem, recent studies based on MD simulations suggested using a voltage ramp that causes the nanopore to switch between its drying or wetting state[13, 22-25]. The modification of the internal wall of the hydrophobic nanopores was also proved to be efficient[11, 26], especially for the

dyalisis method. For instance, Vlassiouk et al. showed that it was possible to control water permeation through the nanopore using light[27] thanks to the functionalization of the nanopore inner wall with photochromic spiropyran and hydrophobic molecules. Whatever the solution offered to improve the ability of water to wet the inner wall of a narrow nanopore, no biological based solution was proposed to solve this fundamental problem.

Gramicidin A (gA), a hydrophobic peptide, forms a transmembrane nanochannel (with a radius smaller than 0.5nm) inside cell membranes, and hence contributes to the cause of the membrane dipole potential[28, 29]. When embedded in a lipid membrane, gA is highly selective to monovalent cations as it allows the transport of water and ions and blocks the passage of divalent cations while its inner radius is very small. Thanks to these properties, the hydrophobicity of the support planar lipid membrane was considerably increased by the incorporation of gA [30].

Recently, we designed small-diameter nanopores with controlled surface states by combining track-etched nanopores and atomic layer deposition (ALD). By accurately controlling the thickness of the deposited film, we were able to produce high aspect ratio hydrophobic nanopores with a length of L = 6 µm and controlled diameters ranging from 1 to 10 nm. However, the smallest diameters were extremely difficult to study due to the sudden apparition of a water vapor phase during experiments and MD simulations[31]. In this paper, we propose to show how hydrophobic polypeptides should overcome these limitations and allow natural wetting of the hydrophobic nanopores. For this purpose, we chose to confine, in ideal controlled conditions, gA inside our narrowest nanopore and show that wetting is restored due to the operation of the gA. This corresponds to a new ultimate biomimetic system that could contribute to the development of experiments for applications. Our biomimetic system could thus be an easy solution for preventing the occurrence of the transition phase both in experimental and theoretical conditions. Our paper is organized as follows. In the first part, the results focus on the transition phases observed in experimental and theoretical raw nanopores. Secondly, the role played by gA is demonstrated, which shows that the wetting of the nanopore is restored in theory and in experiments when the polypeptide is embedded in the nanopore.

RESULTS AND DISCUSSION

Behavior of a bare nanopore

In order to outline the experimental difficulties encountered to fill a hydrophobic nanopore with a small diameter, patch-clamp measurements were firstly performed on a conical hydrophobic nanopore (tip 2 nm, base 590 nm) (Figure 1). The current variations shown in Figure 1 are the consequence of an imperfect and erratic wetting of the nanopore. This phenomenon is typically observed during the filling attempt of the hydrophobic nanopore when current fluctuations appear. They are characteristic of a succession of open and closed states. In order to successfully fill such a narrow hydrophobic nanopore, a high voltage (i.e. electrowetting process[14]) should be applied to the system to force the water molecules to diffuse inside the nanopore. There exists an unstable state, in which the nanopore can be deweted after removing the voltage. Then, after stabilization of the ionic transport process, these current fluctuations are no longer observed when a constant voltage is applied. However, it should be noted that these techniques, involving high voltage applications, are extremely tricky due to the fact that the nanopores could be easily damaged under voltage constraints. In addition, the filling process can require several hours and is attempted before reaching the stable ionic transport state. This depends on the nanopore size and geometry. Basically, a conical nanopore is easier to fill than a cylindrical nanopore.

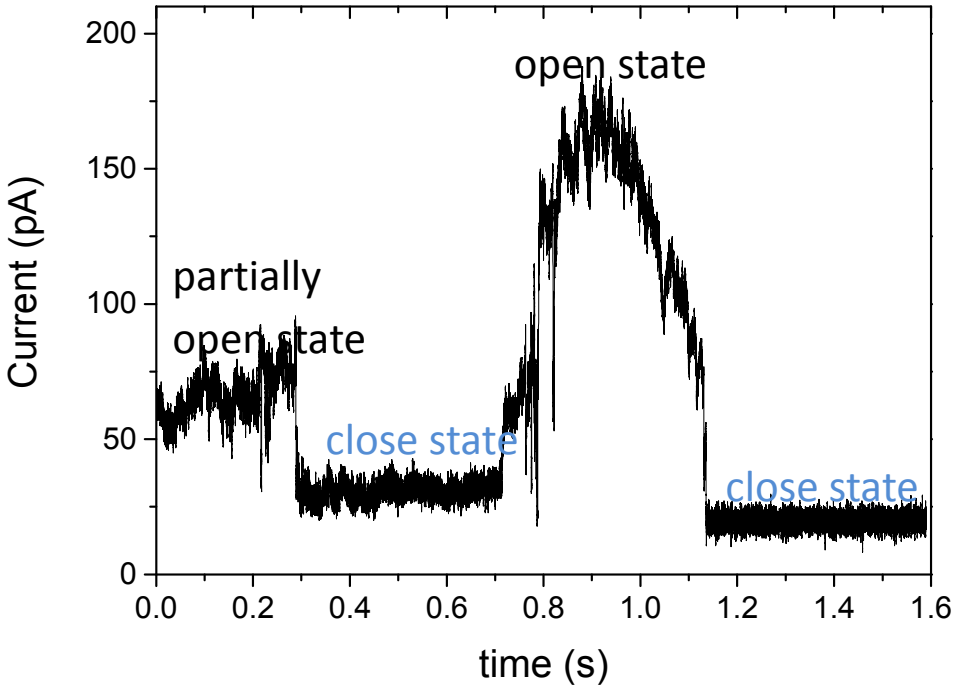

Figure 1: Erratic opening and closing of a trimethyl silane coated conical nanopore (tip 2 nm, base 590 nm). The current graph was recorded under 1 V for NaCl 0.1 M.

In order to study the permeation properties of the narrowest hydrophobic pore (2 nm), we performed molecular dynamic simulations on a nanopore modeled as closely as possible to an experimental nanopore. Different situations were considered. Firstly, all atoms of the nanopore were frozen in the presence of water (with or without ions) to understand the behavior of this "simplest" system. Then, we developed more complicated situations, in which the methyl groups of the nanopore were free to move in the presence of water alone (or with an electrolyte). These simulations were the closest to experimental conditions.

The MD simulations show the major dynamics of confined water. The water density in the pores varies from a value close to the bulk density (filled pore) to a density nearly equal to zero (empty pore) whatever the simulation conditions. For small ion concentrations and a frozen nanopore (Figure 2a), we observed a long period of nanopore wetting (40ns) before a progressive and rapid desorption of the

confined water. Then, a dried state appeared suddenly, which would certainly alternate with a wetting state as observed in experiments (Fig. 1) and in literature. For example, in a highly hydrophobic MscS pore (the small mechanosensitive channel of Escherichia coli) or other biological channels[32], the water occupancy of the constriction region showed repeated transitions between an empty state (~83% of the time) and a filled state[33]. In a narrow carbon nanotube with a radius below 1 nm, these fluctuations were also obtained in simulations. They appeared as a single-file configuration [34, 35] and were confirmed by Hummer et al. [35], who observed that there was a pulse-like transmission of water through the nanotube resulting from the tight hydrogen-bonding network inside the tube. The role of the carbon-water interaction was underlined since it led to sharp, two-state transitions between the empty and filled states in a 25 ns simulation. From an experimental viewpoint, these transitions states were verified by the splitting of the radial breathing mode (RBM) vibration in Raman spectra [36].

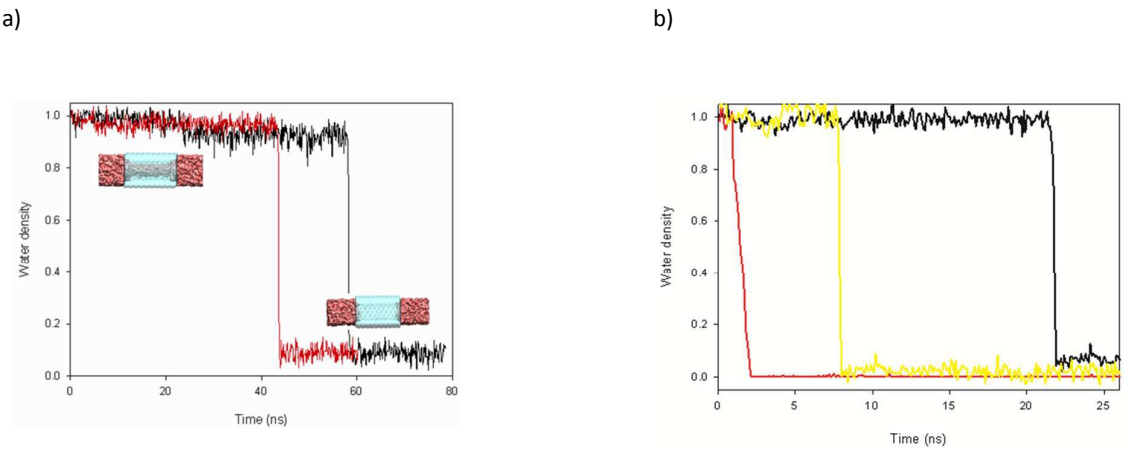

Figure 2: Water density as a function of time for a) a frozen nanopore (the red (black) graph is for an ionic concentration equal to 0.1 M (0.05 M)) and b) a dynamic nanopore (the red (yellow, black) graph is for an ionic concentration equal to 1 M (0.5 M, 0.1 M). The density is measured in units of the bulk water density 0.996 g cm^{-3} at 25°C and the pore diameter is equal to 2 nm.

We can thus see that the dynamics of the nanopore are also of crucial importance in the wetting/dewetting phases. When the methyl groups of the neopentane molecules were left free to

rotate around their central carbon atoms, we observed, in Figure 2b, and for any simulation (low or high ion concentration) that the nanopore was drained more rapidly. In order to highlight the relevance of the NEOP dynamics, we calculated the PMF of a water molecule across the narrow nanopore when it was filled or empty. This observable parameter, defined as the potential giving the average force, in all configurations of all molecules influencing this target water molecule, allowed us to determine the free energy changes according to its coordinate. To calculate the PMF, we progressively pulled the center of mass of the targeted water molecule from one side of the nanopore to the other. The results, shown in Figure 3, demonstrate that the free energy barrier required to penetrate the 2-nm diameter nanotube is much stronger when the nanopore is dynamic (6 kcal mol^{-1}). When the NEOP molecules in the nanopore were kept in a frozen state, the barrier height remained constant during the simulations (1.3 kcal mol^{-1}). Furthermore, the same calculations performed for a nanopore with a greater diameter (3 nm) did not show such significant differences between the dynamic and frozen nanopore walls. The free energy barrier for the insertion of the water molecules in this larger nanopore was approximatively equal to 1.3 kcal mol^{-1} for frozen walls while it slightly increased to 2.2 kcal mol^{-1} for dynamic NEOP molecules. This result corroborates the significance of the flexibility of the hydrophobic methyl function in our simulations when the diameter of the nanopore is small. It is to be noted that the graphite, in which the nanopore was inserted, also contributes to the energy barrier but to a lesser extent.

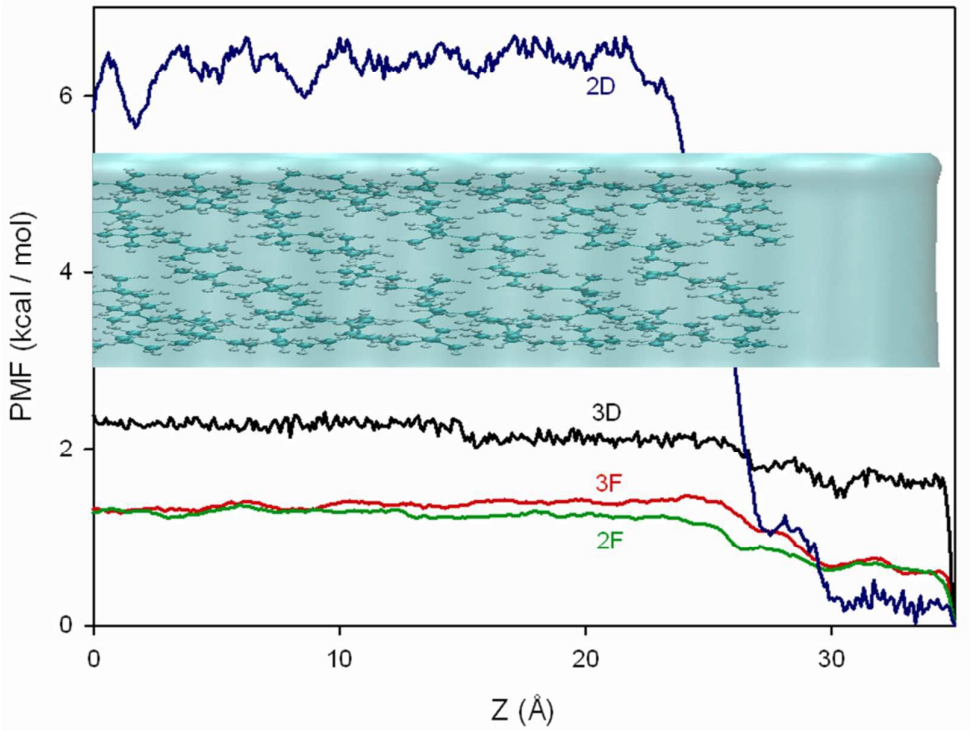

Figure 3: Potential of mean force of one water molecule across the nanotube for different simulation conditions. In blue (black), PMF through a nanopore with a diameter equal to 2 nm (3 nm) and dynamic walls. In green (red), PMF through a nanopore with a diameter equal to 2 nm (3 nm) and frozen walls.

These situations represent a better correspondence to the nanofluidic experiments shown in Figure 1 where the inner ALD nanopore is functionalized with TMS and they explain the long duration of the drying state. It should be noted that the transition state occurs in a shorter time when the ion concentration is increased and that, in literature, water molecules were predicted to be excluded from a pore whose radius was equal to 0.7 nm (at most). In this study, the major dynamics of the hydrophobic pore surface could increase this limit up to 1 nm.

The hydrophobic gating mechanism[12] observed in this study is currently observed in several biological systems and can either be forced or impeded by using external stimuli such as light[27], pressure[23] or voltage[13, 22]. However, in any case, these stimuli significantly damage the fragile

nanopore. Interesting work performed by Guo et al.[37] showed that the modification of the nanopore surfaces by a "chemical" temperature triggered function allowed to control the transition from a close conducting state to an open conducting state with the temperature increase. This experimental work underlined the significant effect that a chemical modification can have on the inner nanopore surface and that it can be used to control the water transition phases. However, no solution against the complete drying phenomenon has been proposed so far for narrow nanopores showing frequent drying states.

The dewetting process observed both experimentally and theoretically within the hydrophobic pore at an applied voltage equal to zero therefore led us to consider a possible 'hydrophobic gating' process within these narrowest pores.

Biomimetic nanopore behavior

The physical solutions proposed to overcome the water transition phase issue could be extremely detrimental for a fragile nanopore with very small diameter. Nevertheless, biological-based solutions may be achieved to make it feasible since bionanochannels known to transport water molecules do exist. In the case of channel proteins, the wetting of their inner media is frequently indispensable to ensure that ions can permeate effectively through them. To be functional, these proteins need to be inserted during their synthesis, into lipid bilayers. For example, membrane proteins, such as toxins[38] and antimicrobial peptides[39], insert themselves into a lipid bilayer without assistance. The insertion mechanism of such proteins, although still poorly understood, is probably lipid-assisted. This mechanism helps one part of the protein to cross the hydrophobic core of the membrane, assists the insertion of the remaining part and then the conduction of the water molecules[40]. The protein channel is currently filled with six water molecules aligned in a single file configuration that allows the monovalent cations to be hydrated. The size of the nanochannel is of about 0.4 nm, which is far from the limited size used in MD simulations to observe hydrophobic gating.

Combining a protein wetting nanochannel with a potent dynamic hydrophobic synthetic nanopore could be an effective solution for preventing water drying. We recently showed that the insertion of a gA protein was possible both experimentally and theoretically as long as it is extracted from the biological media and placed near to the nanopore entrance[41]. The properties of the nanopore were then completely changed in terms of permeability and selectivity, which proved that gA was inserted in the highly hydrophobic nanopore[20]. A successful insertion is affected by many factors such as the nature of the solvent in which gA is dissolved and the size of the nanopore. To optimize the insertion, theoretical investigations were conducted to determine the minimal pore diameter for which the gA could lose its properties. The accommodation of the polypeptide was thus studied within the range of accessible diameters. With large diameter nanopores (>3nm), changes affecting the proteins in terms of size and shape were observed until reaching a minimal gA concentration for which the nanopore wall could no longer roughly influence the gA structure. For smaller diameters, the gA structure was extremely modified depending on the diameter. Several diameters were then tested and, based on a data analysis, a range of diameters between 1.7 to 2.3 nm was determined, in which gA could maintain a stable beta helix structure. gA could thus be inserted into the narrowest drying nanopore (2 nm) in order to study its influence on the behavior of water.

Following the insertion of gA, we examined the stability of the beta helix in terms of energy and structural resolution and established that the polypeptide structure was stabilized when it was maintained inside the hydrophobic nanopore. The upper limit value of the RMSD reached 2.3 Å. This was assigned to the mobility of the gA extremities, which, in principle, are in contact with the lipid head[42, 43]. To demonstrate this point, the RMSD of the two extreme tryptophan groups was plotted in Figure 4. The large displacements of the tryptophan groups (each of them being reflected on the RMSD of the total protein) were due to a strong interaction with the pore wall and with the water molecules to attract them towards the inner nanochannel. It is to be noted that, inside the membrane cell, the structure of the gA was only changed by 1.2 Å with respect to its crystallographic structure[44]. However, the energy of the gA did not vary significantly when the gA was inserted inside the pore due to the fact that its interaction with the dynamic pore wall seems to mimic at best the biological media.

However, the gA structure was modified as it lost its natural folding with 62% of the remaining beta helix, compared to 82% in a lipid environment[44]. This outcome can be considered as satisfactory since the pore wall structure is fairly rigid compared to lipid bilayers.

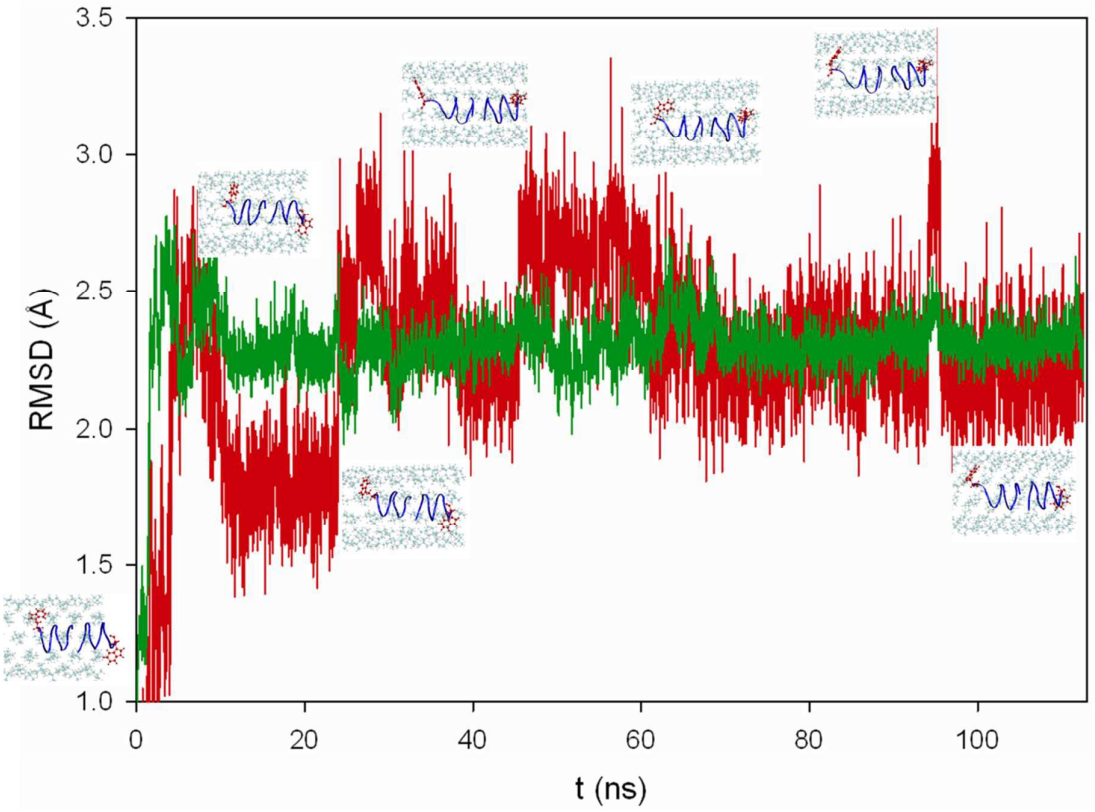

Figure 4: Root Mean Square Deviation of the confined gA during the molecular dynamic simulations in the nanopore. In green (red), RMSD of a full gA structure (only extreme tryptophan Trp-15 groups of gA).

Simulations were thus carried out in the worst-case conditions, in which the drying phase occurred the most frequently, i.e. dynamic pore wall and ionic concentration equal to 1 M. In these conditions (and also other conditions), the water was observed to progressively fill the hydrophilic gA nanochannel, in the continuity of the hydrophobic drying nanopore. Figure 5 shows the progressive

amount of water that fills the biomimetic nanopore as from the start of the simulation. When the gA was inside the hydrophobic nanopore, the electric field generated by the polypeptides counterbalanced the high hydrophobicity of the nanopore and very rapidly attracted the water molecules inside the nanopore.

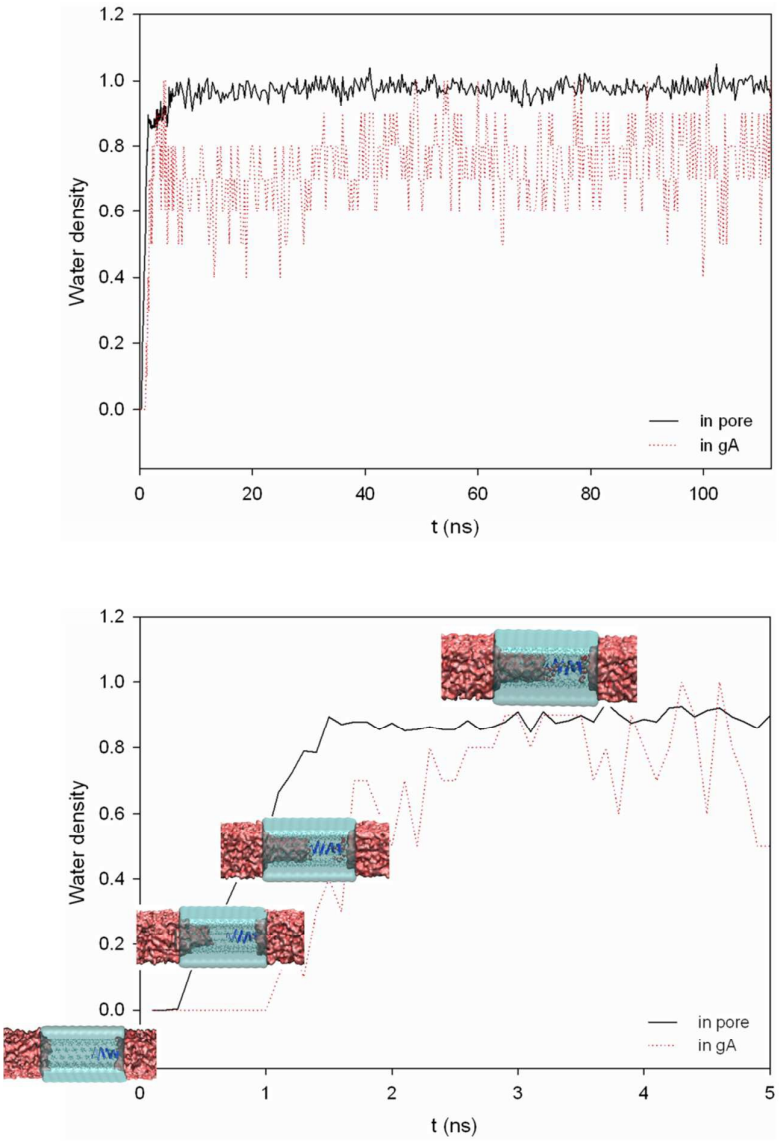

Figure 5: Water density (inside the pore (black curve) and inside gA (red curve)) as a function of the simulation time for the entire duration of the simulation (top). Zoom after a short simulation time and snapshots of the water behavior inside the system (bottom). The water density inside gA was calculated assuming a perfect cylindrical volume (length 2.5 nm and radius 0.2 nm).

The gA folding can only be maintained if a few water molecules fill the nanochannel and form a molecular chain that reduces the electrostatic interactions. Without water, the protein will quickly unfold. We have therefore obtained an effective water pumping device due to the biomimetic transformation of the narrowest nanopore. To confirm this pump effect, we plotted, in Figure 6, the PMF of a water molecule inserted inside the nanopore at the opposite side of the gA. As clearly shown, the free energy barrier, which was equal to 6 kcal mol^{-1} before the gA insertion (Fig. 3), decreased significantly down to 1.2 kcal mol^{-1}. This barrier could be separated into two parts. One part came from the insertion of the water molecule inside the graphite wall and the second part corresponded to the confinement of the molecule inside the nanopore. Simulations were continued up to 300 ns and no wetting/dewetting transition was observed. The variation of the water density inside the nanopore and the nanochannel clearly showed that the two cavities filled progressively during the simulation. This is an efficient way of preventing the drying of a nanopore.

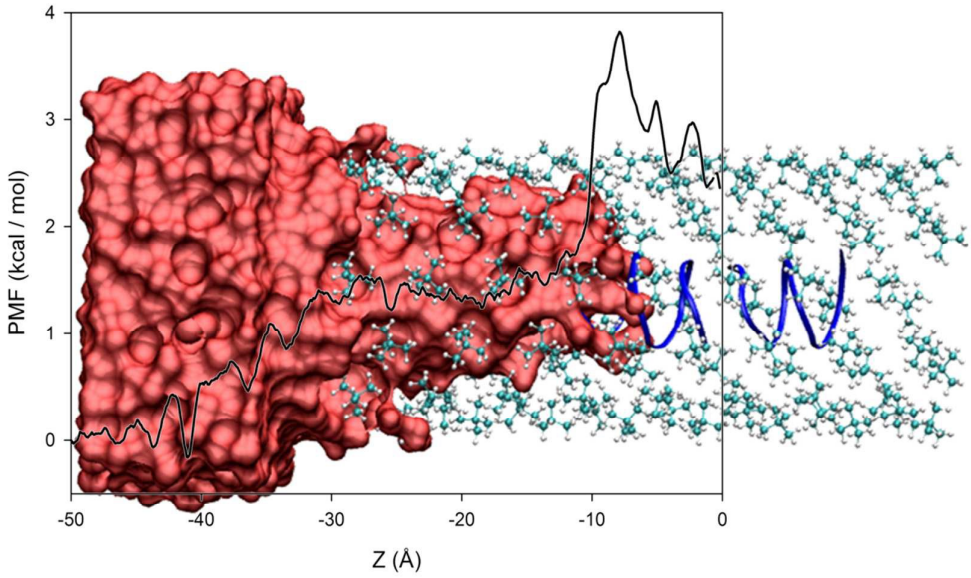

Figure 6: Potential of mean force of one water molecule across the biomimetic nanopore which is depicted behind (only for the PMF limits, i.e. -50<z<0 Å). In black, the PMF shows two barriers. The first one is for the insertion inside the graphite (-40<z<-33 Å) and the second for the insertion inside the nanopore (-33<z<-25 Å).

To experimentally demonstrate these exciting theoretical findings, a gA (100 nM) solution impregnated the nanopore during 72h at 6°C and was confined inside the hydrophobic nanopore. Unfortunately, experimental evidence of our simulation predictions were not achieved in the narrowest nanopore. The insertion of gA inside a conical nanopore (tip diameter 14 nm) was only controlled and demonstrated in a stable current phase. In other words, to fill the nanopore with gA, it should firstly be filled with water. In addition, the differences in the electrical behavior between an unfunctionalized nanopore and a gA-impregnated nanopore were not sufficiently significant to claim that gA has any effect. The ability of the gA insertion inside the smallest hydrophobic nanopore was demonstrated in cylindrical nanopores, in which the conductance differences were at least five times higher than for small nanopores (diameter 2 nm). [20] As long as the gA was inserted inside the narrowest nanopore, no current fluctuations were observed in our experiment (Figure 7). This certainly does not prove the concept but it does not contradict our theoretical investigations.

a) (b

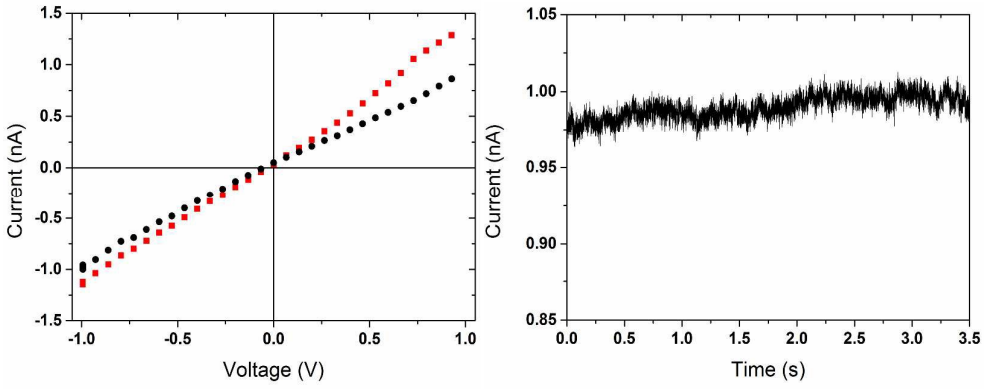

Figure 7: Illustration of the influence of gA on the current for a hydrophobic nanopore (tip 14 nm, base 340 nm) (a) I-V response (KCl 0.1 M) of a nanopore before (red square) and after the gA insertion (black circle) (b) Stable current (record under 1V for KCl 0.1 M) obtained through a nanopore after gA confinement.

CONCLUSION

The smallest hydrophobic nanopore, studied both in experiments and in simulations in this paper, showed a rapid wetting/dewetting transition. This phenomenon was explained in the simulations by the dynamics of the elementary constituents of the nanopore and the role of the ionic concentration in the cavities, which only delayed the occurrence of the transition phase. As already underlined, these transition phases could play a dramatic role due to the fact that the external force required to wet the nanopore could cause its rapid destruction. In this paper, we proposed a simple biological solution which involves inserting a gA nanochannel inside this narrow hydrophobic nanopore. When this insertion is performed, the nanopore remains, even in the worst experimental conditions, fully hydrated and does not undergo any drying phase. Our work, which was fully demonstrated by molecular dynamic simulations and partially achieved experimentally due to technical limitations, shows that by using the properties of biological molecules, a biomimetic functionalization could prevent nanotechnological instruments from dewetting without any external physical stimuli. This study is a successful attempt, which shows that the combination of biological and physical techniques can provide very interesting results.

Materials and methods

Molecular simulations

We performed complete atomistic molecular dynamic (MD) simulations using NAMD 2.9b2 software [45] while respecting a constant temperature of 300 K (Langevin dynamics) and a constant pressure of 1 atm. The Langevin piston Nosé-Hoover method[46] was used to create these experimental conditions. The short- and long-range forces were calculated every 1 and 2 time-steps, respectively, i.e. 1.0 fs, while the long-range electrostatic forces were estimated with the standard particle mesh Ewald (PME) approach[47]. Chemical bonds between the hydrogen and heavy atoms were constrained to their equilibrium value.

All systems (ions, water, membrane, gA) were modeled using the CHARMM27[48] force field. The water molecules were simulated in the TIP3P model. The experimental nanopore was simulated by agglomerating neopentane molecules (NEOP) in a tubular geometry. The central carbon atoms of NEOP were maintained in a bound configuration while the methyl groups forming each molecule were frozen or free to move, depending on the simulations. The mean distance between the fixed centers of mass of the neopentane molecules is chosen according to the work of Makowski *et al.*.[49] This nanopore was then incorporated into a graphite bulk where a hole was created initially. The narrowest diameter (nearly equal to 2 nm and noted NT2 with a length equal to 5 nm) was studied in this case as it corresponds to the most problematic system. The entire system (containing the nanopore) was finally placed between two cavities of 3-nm long, filled with electrolytes with different ionic concentrations in order to study the role of the ions on the nanopore wetting process. For the biomimetic system construction, we chose the monomeric gA conformation[50] (PDB code: 1JNO), which is the equilibrium geometry adopted in bulk water [51]. The gA monomers were firstly pre-equilibrated for at least 5 ns and then inserted into the unfilled nanopore.

Different simulations were performed using high or low ion concentrations. A total cumulated simulation time of 300 ns was used to achieve the best operating conditions for our biomimetic system so as to prevent the occurrence of the wetting/dewetting transition phase.

The free energy profiles were computed using the adaptive biasing force (ABF) method [52, 53], as implemented in NAMD. For all the ABF simulations, the chosen reaction coordinate was the distance between the center of mass of the nanopore (or gA) and the target water molecule, projected on the Z-axis (relative to the nanopore main axis). The channel permeation pathway ($-40\ \text{Å} \le Z \le 0\ \text{Å}$) was subdivided into four non-overlapping windows. The length of each window was 10.0 Å, in which MD were performed for 50 ns, thus resulting in a total simulation time of 200 ns. A 100 kcal $mol^{-1}Å^{-2}$ boundary force constant was applied to restrain the motion of the water molecule of interest inside the window. Each window was sampled with a step size of 0.1 Å and the free energy profile was determined by integrating the average force over all windows. The initial configurations for each

window were taken from intermediate structures of MD simulations, in which the target water molecule was positioned near to the next window. The biasing force was applied only after the accumulation of 1000 samples in a bin beforehand. During all ABF simulations, the motion of the water molecule being considered was limited to a cylinder of 8 Å on the XY directions relative to the main axis of the nanopore.

Nanopore preparation and characterization

Track-etching nanopore

Single conical nanopores were tailored by using a track-etched method [54] and modified by using atomic layer deposition[20]. Basically, the single tracks were produced by Xe irradiation (8,98 MeV u^{-1}) of PET film (13 μm) (GANIL, SME line, Caen, France). Then the track was activated under a 24 h UV exposition per side, (Fisher bioblock; VL215.MC, λ = 312 nm). The chemical etching was performed in assymmetric conditions: the NaOH solution (9 M) was placed on one side of the cell and the stopping solution (1 M KCl) and 1M of acetic acid on the other side of the cell. After the echting process, the diameter of the tip, d_t, of the conical nanopore of length L was estimated from the conductance measurement using equation 1:

$$G = \kappa \pi d_b d_t / 4L \qquad (1)$$

Where d_b was calculated according to the total etching time t providing that $d_b = 2.5t$. The factor 2.5 was determined in the lab by using a mutlipore track membrane. Then the tip diameter of the nanopore was adjusted to 2 nm by deposition of successive Al_2O_3 and ZnO layers according to the so-called atomic layer deposition process using a custom-made setup.[31] Finally, the nanopore was exposed to hexamethyldisilazane (HMDS) to obtain hydrophobic Tri(Methyl-Silane) (TMS) function ($(CH_3)_3Si–$) surface terminal group. To characterize the nanopore, an I-V plot was recorded under NaCl 100mM (Figure 8a). After chemical etching, the I-V graph showed a current rectification due to the carboxyl groups induced by chemical etching. After modification by ALD and HMDS

functionalization, we observed a current decrease and the disappearance of the current rectification, which confirms that the surface is not charged.

To check the hydrophobicity induced by HDMS functionalization, the contact angle was measured on the PET surface functionalized following the same procedure as for the nanopore (Figure 8b). In this case, we measured an angle equal to 92 degrees, which is higher than 90 degrees, the lowest value for hydrophobicity.

a) (b

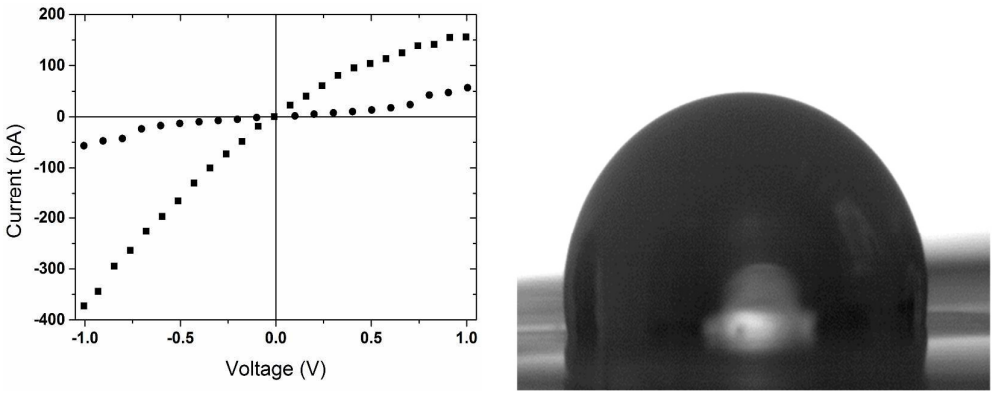

Figure 8: Experimental characterization of the nanopore (tip 2 nm, base 590 nm) (a) I-V response obtained under KCl 100mM before (black square) and after (black circle) ALD and HMDS coating. (b) Contact angle of the PET surface after ALD and HMDS coating.

Current measurement

The current was recorded by using a patch-clamp amplifier (EPC10 HEKA electronics, Germany) as a function of time under applied voltages from 1V. The single nanopore is placed between two Teflon chambers containing the NaCl 0.1 M solution. The current is measured by Ag/AgCl, 1M KCl electrodes connected to the cell chamber by agar-agar bridges. Data was recorded at 200 kHz by using Patchmaster software (Heka Elektronik, Germany). Recorded currents were then analyzed by Fitmaster (Heka Elektronik, Germany).

Conflict of Interest: The authors declare no competing financial interest

Acknowledgements

G. P. gratefully acknowledges the support provided by Prof. Tijani Gharbi through fellowship grant SAIC/2010-77-2 awarded by the Nanomedicine Laboratory. This work was supported in part by the French Research Program ANR-BLANC, Project TRANSION (ANR-2012-BS08-0023). Single tracks have been produced in GANIL (Caen, France) in the framework of an EMIR project. The calculations were carried out with the supercomputer regional facility, Mesocenter, of the University of Franche-Comté. V. Tangaraj has a fellowship of the UE Svaagata program.

References

1. A. Anishkin and S. Sukharev, *Biophys J.*, 2004, **86**, 2883–2895.
2. K. A. Dill and H. S. Chan, *Nat. Struct. Biol.* , 1997, **4**, 10–19.
3. K. Murata, K. Mitsuoka, T. Hirai and e. al., *Nature*, 2000, **407**, 599–605.
4. M. A. Shannon, P. W. Bohn, M. Elimelech, J. G. Georgiadis, B. J. Marinas and A. M. Mayes, *Nature*, 2008, **452**, 301-310.

5. J. R. Bontha and P. N. Pintauro, *Chem Eng Sci*, 1994, **49**, 3835-3851.

6. J. Geng, K. Kim, J. Zhang, A. Escalada, R. Tunuguntla, L. R. Comolli, F. I. Allen, A. V. Shnyrova, K. R. Cho, D. Munoz, Y. M. Wang, C. P. Grigoropoulos, C. M. Ajo-Franklin, V. A. Frolov and A. Noy, *Nature*, 2014, **514**, 612-615.

7. C. Y. Lee, W. Choi, J. H. Han and M. S. Strano, *Science*, 2010, **329**, 1320-1324.

8. A. Siria, P. Poncharal, A. L. Biance, R. Fulcrand, X. Blase, S. T. Purcell and L. Bocquet, *Nature*, 2013, **494**, 455-458.

9. S. Shimizu, M. Ellison, K. Aziz, Q. H. Wang, Z. Ulissi, Z. Gunther, D. Bellisario and M. Strano, *J Phys Chem C*, 2013, **117**, 9641-9651.

10. J. Li, D. Stein, C. McMullan, D. Branton, M. J. Aziz and J. A. Golovchenko, *Nature*, 2001, **412**, 166-169.

11. M. Pevarnik, K. Healy, M. Davenport, J. Yen and Z. S. Siwy, *Analyst*, 2012, **137**, 2944-2950.

12. O. Beckstein, P. C. Biggin and M. S. P. Sansom, *The Journal of Physical Chemistry B*, 2001, **105**, 12902-12905.

13. M. R. Powell, L. Cleary, M. Davenport, K. J. Shea and Z. S. Siwy, *Nat. Nano.*, 2011, **6**, 798-802.

14. S. N. Smirnov, I. V. Vlassiouk and N. V. Lavrik, *ACS Nano*, 2011, **5**, 7453-7461.

15. O. Beckstein and M. S. P. Sansom, *Proceedings of the National Academy of Sciences of the United States of America*, 2003, **100**, 7063-7068.

16. O. Beckstein and M. S. P. Sansom, *Phys. Biol.*, 2004, **1**, 42-52.

17. J. K. Holt, H. G. Park, Y. Wang, M. Stadermann, A. B. Artyukhin, C. P. Grigoropoulos, A. Noy and O. Bakajin, *Science*, 2006, **312**, 1034-1037.

18. B. J. Hinds, N. Chopra, T. Rantell, R. Andrews, V. Gavalas and L. G. Bachas, *Science*, 2004, **303**, 62-65.

19. A. Srivastava, O. N. Srivastava, S. Talapatra, R. Vajtai and P. M. Ajayan, *Nat. Mater.*, 2004, **3**, 610-614.

20. A. Abou Chaaya, M. Le Poitevin, S. Cabello-Aguilar, S. Balme, M. Bechelany, S. Kraszewski, F. Picaud, J. Cambedouzou, E. Balanzat, J.-M. Janot, T. Thami, P. Miele and P. Dejardin, *The Journal of Physical Chemistry C*, 2013, **117**, 15306-15315.

21. S. Cabello-Aguilar, A. Abou Chaaya, M. Bechelany, C. Pochat-Bohatier, E. Balanzat, J. M. Janot, P. Miele and S. Balme, *Soft Matter*, 2014, **10**, 8413-8419.

22. D. Bratko, C. D. Daub, K. Leung and A. Luzar, *Journal of the American Chemical Society*, 2007, **129**, 2504-2510.

23. J. Dzubiella, R. J. Allen and J. P. Hansen, *The Journal of Chemical Physics*, 2004, **120**, 5001-5004.

24. S. Smirnov, I. Vlassiouk, P. Takmakov and F. Rios, *ACS Nano*, 2010, **4**, 5069-5075.

25. S. Vaitheeswaran, J. C. Rasaiah and G. Hummer, *The Journal of Chemical Physics*, 2004, **121**, 7955-7965.

26. C. R. Kellenberger, F. C. Pfleiderer, R. A. Raso, C. H. Burri, C. M. Schumacher, R. N. Grass and W. J. Stark, *RSC Advances*, 2014, **4**, 61420-61426.

27. I. Vlassiouk, C.-D. Park, S. A. Vail, D. Gust and S. Smirnov, *Nano Letters*, 2006, **6**, 1013-1017.

28. M. D. Becker, D. V. Greathouse, R. E. Koeppe and O. S. Andersen, *Biochemistry*, 1991, **30**, 8830-8839.

29. A. M. O'Connell, R. E. Koeppe and O. S. Andersen, *Science*, 1990, **250**, 1256.

30. W. B. Han, Y. Kim, H. H. An, H.-S. Kim and C. S. Yoon, *The Journal of Physical Chemistry B*, 2014, **118**, 3035-3040.

31. S. Balme, F. Picaud, M. Manghi, J. Palmeri, M. Bechelany, S. Cabello-Aguilar, A. Abou-Chaaya, P. Miele, E. Balanzat and J. M. Janot, *Scientific Reports*, 2015, **5**, 10135.

32. P. Aryal, M. S. P. Sansom and S. J. Tucker, *Journal of Molecular Biology*, 2014, **427**, 121-130.

33. A. Anishkin and S. Sukharev, *Biophys J*, 2004, **86**, 2883-2895.

34. H. P. Fang, R. Z. Wan, X. J. Gong and e. al., *J. Phys. D*, 2008, **41**, 103002.

35. G. Hummer, J. C. Rasaiah and J. P. Noworyta, *Nature*, 2001, **414**, 188–190.

36. S. Cambré, B. Schoeters, S. Luyckx and e. al., *Phys. Rev. Lett.*, 2010, **104**, 207401.

37. W. Guo, H. W. Xia, F. Xia and e. al., *Chem. Phys. Chem.*, 2010, **11**, 859–864.

38. E. Gouaux, *Curr Opin Struct Biol*, 1997, **7**, 566-573.

39. S. H. White, W. C. Wimley and M. E. Selsted, *Curr Opin Struct Biol*, 1995, **5**, 521-527.

40. A. Aksimentiev and K. Schulten, *Proceedings of the National Academy of Sciences of the United States of America*, 2004, **101**, 4337-4338.

41. S. Balme, J. M. Janot, L. Berardo, F. Henn, D. Bonhenry, S. Kraszewski, F. Picaud and C. Ramseyer, *Nano Letters*, 2011, **11**, 712-716.

42. W. Hu and T. A. Cross, *Biochemistry*, 1995, **34**, 14147-14155.

43. R. E. Koeppe, J. A. Killian and D. V. Greathouse, *Biophysical Journal*, 1994, **66**, 14-24.

44. F. Picaud, S. Kraszewski, C. Ramseyer, S. Balme, P. Dejardin, J. M. Janot and F. Henn, *Physical Chemistry Chemical Physics*, 2013, **15**, 19601-19607.

45. J. C. Phillips, R. Braun, W. Wang, J. Gumbart, E. Tajkhorshid, E. Villa, C. Chipot, R. D. Skeel, L. Kalé and K. Schulten, *Journal of Computational Chemistry*, 2005, **26**, 1781-1802.

46. S. Feller, *J. Chem. Phys.*, 1995, **103**, 4613.

47. T. Darden, D. York and L. Pedersen, *J. Chem. Phys.*, 1993, **98**, 10089-10092.

48. A. D. MacKerell, D. Bashford, Bellott, R. L. Dunbrack, J. D. Evanseck, M. J. Field, S. Fischer, J. Gao, H. Guo, S. Ha, D. Joseph-McCarthy, L. Kuchnir, K. Kuczera, F. T. K. Lau, C. Mattos, S. Michnick, T. Ngo, D. T. Nguyen, B. Prodhom, W. E. Reiher, B. Roux, M. Schlenkrich, J. C. Smith, R. Stote, J. Straub, M. Watanabe, J. Wirkiewicz-Kuczera, D. Yin and M. Karplus, *The Journal of Physical Chemistry B*, 1998, **102**, 3586-3616.

49. M. Makowski, C. Czaplewski, A. Liwo and H. A. Scheraga, *J Phys Chem B*, 2010, **114**, 993-1003.

50. R. Ketchem, W. Hu and T. Cross, *Science*, 1993, **261**, 1457-1460.

51. D. Bonhenry, S. Kraszewski, F. Picaud, C. Ramseyer, S. Balme, J. M. Janot and F. Henn, *Soft Matter*, 2011, **7**, 10651-10659.

52. E. Darve, D. Rodriguez-Gimez and A. Pohorille, *The Journal of Chemical Physics*, 2008, **128**, 144120.

53. D. Rodriguez-Gomez, E. Darve and A. Pohorille, *The Journal of Chemical Physics*, 2004, **120**, 3563-3578.

54. M. Lepoitevin, G. Nguyen, M. Bechelany, E. Balanzat, J.-M. Janot and S. Balme, *Chemical Communications*, 2015, **51**, 5994-5997.